Relationship between Quantitative Adverse Plaque Features from Coronary CT Angiography and Downstream Impaired Myocardial Flow Reserve by ^{13}N-Ammonia Positron Emission Tomography: A Pilot Study

Damini Dey, PhD[1], **Mariana Diaz Zamudio, MD**[2], **Annika Schuhbaeck, MD**[3], **Luis Eduardo Juarez Orozco, MD**[4], **Yuka Otaki, MD**[2], **Heidi Gransar, MSc**[2], **Debiao Li, PhD**[1], **Guido Germano, PhD**[2], **Stephan Achenbach, MD**[3], **Daniel S. Berman, MD**[2], **Aloha Meave, MD**[4], **Erick Alexanderson, MD**[4,5], and **Piotr J. Slomka, PhD**[2]

[1]Biomedical Imaging Research Institute, Cedars-Sinai Medical Center, Los Angeles, CA

[2]Department of Imaging and Medicine, Cedars-Sinai Medical Center, Los Angeles, CA

[3]Department of Cardiology, University of Erlangen, Erlangen, Germany

[4]Universidad Nacional Autonoma de Mexico and Instituto Nacional de Cardiologia Ignacio Chavez, Mexico, DF, Mexico

[5]Unidad PET/CT Ciclotron Facultad de Medicina UNAM, Mexico, DF, Mexico

Abstract

Background—We investigated the relationship of quantitative plaque features from coronary CT Angiography (CTA) and coronary vascular dysfunction by impaired myocardial flow reserve (MFR) by ^{13}N-Ammonia Positron Emission Tomography (PET).

Methods and Results—Fifty-one patients (32 men, 62.4±9.5 years) underwent combined rest-stress ^{13}N-ammonia PET and CTA scans by hybrid PET/CT. Regional MFR was measured from PET. From CTA, 153 arteries were evaluated by semi-automated software, computing arterial non-calcified plaque (NCP), low-density NCP (NCP<30 HU), calcified and total plaque volumes,

Correspondence to: Dr. Damini Dey, Phone: 310-423-1517, Damini.Dey@cshs.org, Address: Cedars-Sinai Medical Center, Taper Imaging Rm A238, 8700 Beverly Blvd, Los Angeles CA 90048.

and corresponding plaque burden (plaque volumex100%/vessel volume), stenosis, remodeling index, contrast density difference (maximum difference in luminal attenuation per unit area in the lesion), and plaque length. Quantitative stenosis, plaque burden and myocardial mass were combined by boosted ensemble machine-learning algorithm into a composite risk score to predict impaired MFR (MFR 2.0) by PET, in each artery. Nineteen patients (37%) had impaired regional MFR in at least one territory, (41/153 vessels). Patients with impaired regional MFR had higher arterial NCP (32.4 vs.17.2 %), low-density NCP (7 vs 4 %) and total plaque burden (37 vs 19.3 %, p<0.02). In multivariable analysis with 10-fold cross-validation, NCP burden was the most significant predictor of impaired MFR (Odds Ratio 1.35, p=0.021). For prediction of impaired MFR with 10-fold cross-validation, receiver-operating-characteristics-area-under-the-curve for the composite score was 0.83 (95%CI:0.79–0.91), greater than for quantitative stenosis (0.66, 95%CI: 0.57–0.76, p = 0.005).

Conclusions—Compared to stenosis, arterial NCP burden and a composite score combining quantitative stenosis and plaque burden from CTA significantly improves identification of downstream regional vascular dysfunction.

Keywords

noncalcified plaque; plaque volume; plaque burden; stenosis; coronary CT angiography; impaired myocardial flow reserve; vascular dysfunction; ^{13}N-Ammonia PET

Subject Terms

Nuclear Cardiology and PET; Computerized Tomography (CT)

Coronary Computed Tomography Angiography (CTA) allows direct noninvasive assessment of coronary artery disease, over the coronary artery tree [1–5]. In addition to luminal stenosis, CTA also permits assessment of atherosclerotic plaque, including plaque burden, distribution, and composition, and coronary artery remodeling, previously only achievable through invasive means[6–10]. Impaired Myocardial Flow Reserve (MFR), defined as the ratio of hyperemic myocardial blood flow to that at rest, is known as an imaging marker of prognostic importance[11–14]. The aim of this study was to investigate whether automated measurements of coronary plaque burden can predict coronary vascular dysfunction by impaired MFR measured by ^{13}N-Ammonia Positron Emission Tomography (PET), and further, to evaluate the feasibility of an objective machine learning approach to predict coronary vascular dysfunction by combining multiple quantitative plaque features from CTA.

Methods

Patients

The study sample consisted of consecutive patients with suspected CAD referred for combined noninvasive evaluation of myocardial perfusion by rest-stress ^{13}N-Ammonia PET and anatomical coronary evaluation by CTA, from July 2010 to October 2012. Patients with known hypersensitivity to beta-blockers and iodinated contrast agents, patients with renal failure (serum creatinine level > 1.2 mg/dL), and patients with contraindications for

adenosine administration were excluded from imaging. Sixty-six patients were referred for combined PET-MPI and CTA. 8 patients had coronary stents and were excluded for quantitative plaque analysis. Further, 7 patients had significant motion artifacts on CTA, due to which at least one coronary artery was judged to have non-evaluable segments. These patients were excluded from analysis. Our study included 51 patients (32 men, age 62.4 ± 9.5 years). Table 1 shows the characteristics of the patients in this study. The study was approved by the Institutional Review Board and the subjects gave informed consent.

Hybrid PET/CT acquisition and reconstruction

All images were acquired on a whole-body 64-slice PET/CT scanner (Biograph True Point; Siemens Medical Solutions). PET data were acquired in 3-dimensional list mode. Patients were studied after an overnight fast, and all refrained from caffeine-containing beverages or theophylline-containing medications for 24 h before the study. Myocardial perfusion was assessed at rest and during vasodilator stress with adenosine and ^{13}N-Ammonia as a perfusion radiotracer. Two CT-based transmission scans (120 kVp; 20–30 mA; helical scan mode with a pitch of 1.35) were obtained before the rest perfusion studies and after the stress perfusion studies with normal breathing, for correction of photon attenuation for PET. The registration of the CT attenuation map with the PET images was verified visually by an experienced technologist, and alignment was corrected if necessary by manual 3D translation. Regional myocardial perfusion was first assessed during rest using 740 MBq of ^{13}N-Ammonia. Rest imaging extended for 10 min and began a few seconds before the ^{13}N-Ammonia injection. The ^{13}N-Ammonia was administered as a single peripheral intravenous bolus (3–5 s), followed by a 10-mL saline flush. Thirty minutes later, a pharmacologic stress test was performed, beginning with the injection of adenosine during a 6-min period (140 mg/kg/min). A second dose of 740 MBq of ^{13}N-Ammonia was injected at the third minute of the adenosine infusion. Stress image acquisition was started a few seconds before the radiotracer injection. Sixteen dynamic frames were reconstructed (twelve 10-seconds, two 30-seconds, one 1-minute, and one 6-minute frames, for a total of 10 min). Standard reconstruction (2-dimensional attenuation-weighted ordered-subsets expectation maximization) was used with 3 iterations and 14 subsets and 3D post filtering with a 5-mm Gaussian kernel filter. Transverse data were reformatted to a $168 \times 168 \times 47$ matrix with 2-mm pixels for each dynamic frame.

CTA was performed with the 64-slice PET/CT scanner (Biograph True Point; Siemens Medical Solutions) without changing the patient position on the imaging table. Before CT imaging, patients with a heart rate >70 bpm were given metoprolol (up to 100 mg oral or 20 mg intravenous in 5 mg increments) to attain a heart rate <70 bpm. A short-acting nitrate (5 mg of isosorbide dinitrate) was given to all patients 2–3 minutes before the scan. For CTA, after a timing bolus, ECG-gated helical scanning was performed using ECG-based dose modulation whenever possible, and administration of 60–80 mL of Iopamiron 370 (370 mg iodine/mL, rate 5 mL/second, Schering Bayer, Germany) during a 10-second breath-hold. Scan parameters included heart rate-dependent pitch (range: 0.18–0.2), 330-ms gantry rotation time, 120 kVp tube voltage and tube-current time product ranging between 550–945 mAs. Filtered backprojection reconstruction of contrast enhanced data were performed at end-systole and in diastole with the use of the following parameters: 0.6 mm slice thickness,

0.3-mm slice increment, 250-mm field of view, 512×512 matrix, and a "medium smooth" kernel. The cardiac phase with the best image quality was used for further analysis. Reconstructed CTA images were reviewed and analyzed by an expert reader blinded to PET data.

Quantification of MFR by PET

Global and regional myocardial blood flow values in mL/g/min and MFR values were derived from PET using automated QPET software, as described previously [15]. Left ventricular contours were determined automatically from summed dynamic image data, skipping the first 2 min [15]. The region for the left ventricular input function was automatically placed in the middle of the valve plane and was cylindrical with a 1-cm radius and 2-cm length, with its long axis oriented along the long axis of the heart; left ventricular contours and input function placement were reviewed by an expert reader who was blinded to CTA. Dynamic myocardial samples were obtained from the polar map, by analyzing all time frames within the fixed left ventricular contour boundaries. Using a standard 2-compartment kinetic model for ^{13}N-Ammonia [16][15], stress and rest flow values in mL/g/min were computed for each sample on the polar map as previously described [15]. MFR was computed as a ratio, by dividing each stress polar map sample by the rest samples at each point. The MFR values were corrected by adjusting the resting flow by the resting pressure product, following standard processing technique, in QPET. The total MFR stress and rest flow was computed within the whole LV region bounded by the LV plane. The regional flow was then obtained by dividing the polar map into three regions (left anterior descending artery, left circumflex coronary artery, and right coronary artery) from the standard 17-segment American Heart Association model. Regional and global MFR values were extracted automatically for further analysis. Regional MFR 2.0 was considered impaired, as validated in prognostic studies. For stress flow, from quantitative ^{13}N-Ammonia PET data of 18 low-likelihood patients with no chest pain imaged at the same center, with normal PET perfusion and function, a threshold of 2.0 mL/g/min was considered to be hyperemic [15].

Coronary CTA analysis

Assessment of multiple plaque characteristics in the coronary arteries was performed with a previously developed automated algorithm (AutoPlaq). Several quantitative measurements were made over each coronary artery up to a normal (reference) arterial diameter limit 1.5 mm. [17, 18] To quantify coronary artery segments with any plaque, coronary CTA images were examined in multiplanar format and proximal and distal limits of the plaque lesions were manually marked by an experienced reader blinded to PET data; plaque lesions with all levels of stenosis were included. Subsequent plaque quantification was fully automated using adaptive algorithms that are scan specific. [17, 18] Quantitative percent stenosis was calculated by dividing the narrowest lumen diameter by the mean of two normal non-diseased reference points. The absolute volumes for total plaque, non-calcified plaque and calcified plaque were computed using scan-specific thresholds, as previously described. [17, 18] Low-density non-calcified plaque was defined as non-calcified plaque below a preset low-density threshold (30 HU).[19] The plaque burden for each of these plaque components was calculated, defined as the plaque volume normalized to the vessel volume (plaque volume $\times$ 100%/vessel volume). Remodeling index was determined as the ratio of

maximum vessel area to that at the proximal normal reference point.[7] Lesion length (in mm) was the length of the diseased vessel as computed in Autoplaq. Contrast density difference over the lesion, was computed as follows: the luminal contrast density, defined as attenuation per unit area, similar to "area gradient",[20] was computed over 1 mm cross-sections of the arterial segment. The contrast density difference was defined as the maximum percent difference in contrast densities, with respect to the proximal reference cross-section (with no disease). For each artery, maximum diameter stenosis, remodeling index and contrast density difference values were reported. The CTA images were evaluated with and without plaque overlay, using transverse and MPR views. In MPR views, longitudinal views and short axis views of each segment were visually assessed, with and without plaque overlay, as previously described [18, 21]. If the vessel wall needed adjustment, minor edits were made using the automated vessel wall correction options in the software.

Composite Risk Score by machine learning

For the composite risk score by machine learning, we employed an ensemble-boosting machine learning algorithm, which is a meta-algorithm technique. In ensemble boosting, a high performance of classification is obtained by combining individual classifiers, resulting in a strong ensemble classification scheme by iteratively adjusting appropriate weights for each of the base-level classifiers. For the current analysis, we utilized the LogitBoost method [22], which has been shown to be superior to the other methods such as AdaBoost [23, 24][25], and has been successfully applied previously to a variety of classification schemes, including improvement of the diagnostic accuracy of myocardial perfusion Single Photon Emission Computed Tomography (SPECT) [26]. Patient age, gender, quantitative plaque features (maximum stenosis, non-calcified, low-density and calcified plaque burden, total lesion length and contrast density difference) as well as estimated myocardial mass were combined by machine learning into a composite risk score to predict regional impaired arterial MFR (MFR 2.0 by PET) within the Waikato Environment for Knowledge Analysis (WEKA) environment [27]. Since total and non-calcified plaque burden are highly correlated, only characterized plaque burden (non-calcified, low-density non-calcified and calcified) were included in the logistic regression models and in machine learning. Myocardial mass was estimated from multiplying measured myocardial volume with myocardial density (1.05 g/mL). Ten-fold stratified cross-validation technique was applied to ensure that none of the arteries to create the machine learning model was used in subsequent evaluation of the same model for the prediction of impaired MFR. The machine learning score was thus validated on unseen data using standard 10-fold cross validation. Ten-fold cross validation has been shown to have smaller bias for discriminant analysis than traditional split-sample approach (test and validation)[28] and is currently the preferred technique in data mining [27] Following ten-fold cross validation, the final continuous risk scores representing the probability of impaired MFR were derived per-vessel [27]. In our implementation of the 10-fold cross-validation (which was used both for the machine learning composite score and logistic regression) the arteries were always clustered at the patient level, thus in each-fold of the cross-validation there was no patient data where one artery belongs to the training set and the other artery of the same patient to the validation set. This was done to ensure the real life-test of the application, where the method is tested always in new patients and no single patient is used in the training and validation at the same time. For per-patient analysis for the

machine learning score, we applied the maximum composite risk score, similar to maximum diameter stenosis, which has been previously used.

Statistical Analysis

Statistical analyses were performed with STATA software (version 11 StataCorp LP). For all continuous variables, the Shapiro-Wilk test was used to assess normality. All continuous variables were described as mean ± standard deviation, or median and interquartile range (IQR). Two-sample t-tests (or Wilcoxon rank-sum test) were used to compare groups regarding continuous variables, while Pearson Chi-square or Fisher exact test were used to compare groups regarding categorical variables. Since three coronary arteries were examined per patient, the intraclass coefficient was calculated to determine the design effect and the need to adjust these data for clustering, as in a previous study [29]. For any logistic regression, the data from 3 coronary arteries were grouped by clustering. This takes into account that the observations may be dependent within each patient and specifies that the standard errors allow for intragroup correlation [30, 31]. This method has been previously used to group data from 3 vessels.[29] Furthermore, in our study, 10-fold cross-validation was used for all logistic regression, as previously described for machine learning. For multivariable logistic regression analysis, quantitative CTA measures were not normally distributed, and required transformation to logarithmic-scale. A p-value of <0.05 was considered statistically significant and all tests were two-sided. ROC-area under the curve comparisons were done based on the methods of DeLong et al[32].

Results

Median patient age was 61 years (range 42–85). Demographic and clinical characteristics are listed in Table 1. Nineteen out of 51 patients (37%) had impaired regional MFR in at least one territory, in a total of 41 out of 153 vessels. There was no difference in any patient characteristics in the impaired MFR versus normal MFR group, except higher patient age for impaired MFR (66.6 ± 8.9 years versus 59.3 ± 8.2 years, p = 0.008). Thirty-one patients had stress flows < 2.0 mL/g/min, in a total of 66 vessels. There were 30 vessels with epicardial narrowing of 50% of greater, however MFR was impaired in only 14. Regional perfusion defects (defined as regional ischemic total perfusion defect 3% [33]) were present in 29 vessels in 21 patients. Table 2 shows the stress and rest myocardial blood flow in all patients and in patients with impaired and normal MFR.

Quantitative CTA parameters in arteries with impaired vs. normal MFR

Stenosis measures were significantly higher in arteries with impaired compared to normal MFR (Table 3). Patients with significant stenosis had higher frequencies of impaired MFR (14% vs 34%, p=0.006) and stress flow values < 2.0 mL/g/min (4% vs 34%, p<0.001). Arteries with impaired MFR displayed significantly higher total plaque burden (37.0 vs. 19.3%, p=0.007). Similarly, non-calcified plaque and low-density non-calcified plaque burden were significantly higher in vessels with impaired MFR (Table 3). Further, contrast density difference was significantly greater in vessels with impaired MFR (17.9 vs. 8.4%, p=0.006), with a trend towards greater total lesion length (27.5 vs. 14 mm). Remodeling

index was not significantly different. Figure 1 shows a case example from our study for a patient with impaired MFR in the RCA coronary artery.

Table 4 shows univariate prediction of impaired MFR by the quantitative per-vessel adverse plaque features Total number of risk factors and calcified plaque burden were not predictors of impaired MFR. In multivariable analysis with stenosis and non-calcified plaque burden, and lesion length, adjusted by age, and gender, and with clustering of 3 coronary arteries for each patient [29], non-calcified plaque burden was the most significant predictor of coronary vascular dysfunction (Odds Ratio 1.35, p= 0.003, Table 5). Using stepwise logistic regression, when non-calcified plaque was included in the model, quantitative stenosis as well as lesion length were not significant by multivariable analysis (p=0.77 and p=0.96 respectively).

Table 6 shows the Spearman rank correlation of per-vessel quantitative plaque features with continuous values of regional MFR and stress myocardial blood flow. As seen in Table 6, plaque burden measures (noncalcified, low-density noncalcified, calcified and total plaque burden) showed significant negative correlation with MFR and stress myocardial blood flow. As well, stenosis, contrast density difference and lesion length measures show significant negative correlations with MFR and stress myocardial blood flow.

Composite risk score from quantitative CTA

Figure 2 shows the ROC curves for maximal stenosis and the composite score from combining quantitative stenosis and plaque parameters (after 10-fold cross-validation). As seen in Figure 3, there was a significant increase in area-under-the curve for the composite score when compared to maximal stenosis [0.83 (95% CI: 0.79–0.91) vs. 0.66 (95% CI: 0.57–0.76), p=0.005]. In per-patient analysis, the AUC was 0.93 (95% CI: 0.86–1.00), significantly higher than maximum diameter stenosis (0.69, 95% CI: 0.53–0.84), p=0.0016 (Figure 3). At a per-patient composite score threshold of 0.28, determined by the optimal Youden's J-statistic[34], the accuracy, sensitivity, and specificity to determine impaired MFR were 86.3%, 84.2%, and 87.5% respectively.

Discussion

Our results show that automatically measured non-calcified plaque burden in the coronary artery significantly improves prediction of impaired MFR in the corresponding coronary artery territory. Non-calcified plaque burden was the most significant predictor of impaired regional MFR by multivariable analysis. In addition, we showed that an objective score by combining age, gender, stenosis and characterized arterial plaque burden can significantly improve prediction of impaired MFR measured by ^{13}N-Ammonia PET.

Impaired MFR, a noninvasive measure of coronary vascular dysfunction, is an early manifestation of coronary artery disease; its prognostic significance has been well-documented[11–13]. Recent studies have further shown that in symptomatic patients with normal myocardial perfusion imaging by Rb-82 PET, impaired MFR but not the coronary artery calcium score provides significant incremental risk stratification over clinical risk score for prediction of major adverse cardiac events[35] and that in this patient population,

coronary vascular dysfunction predicts adverse outcomes regardless of gender[36]. In a study of 107 patients undergoing PET with ^{15}O-water and coronary CTA and subsequently invasive coronary angiography with FFR, Kajander et al have shown that obstructive stenosis detected by CTA was suboptimal in assessing stenosis severity with a positive predictive value of 81%, and hybrid PET/CT improved detection of coronary artery disease [37]; in that study, plaque characteristics were not assessed or measured. A previous investigation by Naya et al has evaluated the relationship of visually assessed total coronary plaque burden and composition from CTA with impaired regional MFR measured by Rb-82 PET in 73 consecutive patients [38]. In that study, on a per-vessel basis, maximum diameter stenosis (p=0.02) and summed stenosis score (p=0.002) were the best predictors of regional impaired myocardial flow reserve. On a per-patient basis, a modified Duke CAD index integrating the site and severity of coronary stenosis, and number of coronary segments with mixed plaque, were associated with decreased MFR. As discussed by the authors, the latter finding suggested noncalcified plaques may be as a surrogate marker of more diffuse coronary microvascular dysfunction[38]; however, quantitative non-calcified or total plaque burden was not measured in that study. The results of our study are also in line with prior studies investigating the relationship of CTA plaque characteristics with ischemia by PET and SPECT. A study by Shmilovich et al examined the relationship of adverse plaque features - low attenuation plaque identified by expert reader and positive remodeling (remodeling index > 1.1) and spotty calcifications with ischemia, in 49 patients undergoing both CT and myocardial perfusion imaging[33]. Plaques with both low attenuation and positive remodeling were significantly more likely to be associated with ischemia compared to plaques without these features[33]. In a very recent study, in 56 lesions of intermediate stenosis by CTA for consecutive patients who subsequently underwent invasive coronary angiography with FFR assessment, automatically quantified total and non-calcified plaque burden significantly improved prediction of lesion-specific ischemia by FFR, compared to luminal stenosis[39].

Our study with quantitative analysis of both CTA and PET is unique since it investigates the relationship of quantitative plaque measures with impaired MFR by ^{13}N-Ammonia PET, which has not been reported before. Further, our work adds to these studies by inclusion of previously not reported quantitative CTA parameters derived from automated measurement, particularly plaque burden and contrast density difference. Our results show, for the first time, that non-calcified plaque burden, a marker of plaque vulnerability from noninvasive CTA, is significantly related to impaired MFR, also known for its prognostic importance. From a mechanistic point of view, as summarized in [40], the endothelium and its product nitric oxide (NO) are key regulators of vascular health. Flow-mediated and endothelium-dependent release of NO not only causes epicardial vasodilation but also exerts numerous anti-atherosclerotic effects such as prevention of leukocyte migration and low-density lipoprotein deposition in the sub-intimal space, prevention of smooth muscle cell proliferation, as well as anti-oxidative, and anti-inflammatory effects, all of which confer a certain vascular protection. Our finding that non-calcified plaque – a marker of endothelial injury - is an independent predictor of regional microvascular dysfunction, confirms, at least in part, this hypothesis.

Another novel finding of our study is that an objective composite score combining quantitative stenosis and plaque measures from CTA significantly improves prediction of coronary vascular dysfunction. To our knowledge, these results have not been shown before, particularly using ^{13}N-Ammonia PET as reference standard. It is uncommon for symptomatic patients to undergo both CTA and myocardial perfusion imaging simultaneously; typically either one or the other test is performed, as indicated. Our results show that improved prediction of coronary vascular dysfunction may be possible from objective combination of quantitative stenosis and plaque, from anatomical CTA alone. Such objective scores by machine learning may improve risk prediction for the patient from CTA, without additional imaging or radiation risk.

We acknowledge several limitations in our study. A major limitation was that ours was a pilot study of 51 patients with intermediate likelihood of coronary artery disease at a single medical center. Larger studies are therefore necessary to verify the results from this preliminary pilot study. In order to prevent model overfitting given our sample size, we only included univariate analysis in Tables 1–4 and only 3 covariates are included in the multivariable analysis (Table 5). The small number of patients in our study also did not allow further analysis of vascular territories with and without epicardial narrowing of 50%. While ten-fold cross-validation was extensively used in our study for validation, our study lacked an external additional validation cohort, which is needed to verify the validity of the current findings in data from other centers.

In this study, we showed that quantitative plaque characteristics and specifically non-calcified plaque burden, expressed as the percent of the volume of the artery containing non-calcified plaque from CTA, have the potential to aid in identifying downstream regional vascular dysfunction. Our study also shows that an objective composite score combining quantitative stenosis and plaque measures from CTA significantly improves identification of downstream regional vascular dysfunction, over measured stenosis.

Supplementary Material

Refer to Web version on PubMed Central for supplementary material.

Acknowledgments

References

1. Budoff MJ, Dowe D, Jollis JG, Gitter M, Sutherland J, Halamert E, Scherer M, Bellinger R, Martin A, Benton R, Delago A, Min JK. Diagnostic performance of 64-multidetector row coronary computed tomographic angiography for evaluation of coronary artery stenosis in individuals without known coronary artery disease: Results from the prospective multicenter accuracy (assessment by coronary computed tomographic angiography of individuals undergoing invasive coronary

angiography) trial. Journal of the American College of Cardiology. 2008; 52:1724–1732. [PubMed: 19007693]

2. Hausleiter J, Meyer T, Hadamitzky M, Zankl M, Gerein P, DorrLer K, Kastrati A, Martinoff S, Schomig A. Non-invasive coronary computed tomographic angiography for patients with suspected coronary artery disease: The coronary angiography by computed tomography with the use of a submillimeter resolution (cactus) trial. European Heart Journal. 2007; 28:3034–3041. [PubMed: 17540851]

3. Achenbach S, Ropers U, Kuettner A, Anders K, Pflederer T, Komatsu S, Bautz W, Daniel WG, Ropers D. Randomized comparison of 64-slice single- and dual-source computed tomography coronary angiography for the detection of coronary artery disease. J Am Coll Cardiol Cardiovascular Imaging. 2008; 1:177–186.

4. Miller JM, Rochitte CE, Dewey M, Arbab-Zadeh A, Niinuma H, Gottlieb I, Paul N, Clouse ME, Shapiro EP, Hoe J, Lardo AC, Bush DE, de Roos A, Cox C, Brinker J, Lima JAC. Diagnostic performance of coronary angiography by 64-row ct. N Engl J Med. 2008; 359:2324–2336. [PubMed: 19038879]

5. Meijboom WB, van Mieghem CAG, Mollet NR, Pugliese F, Weustink AC, van Pelt N, Cademartiri F, Nieman K, Boersma E, Jaegere Pd, Krestin GP, de Feyter PJ. 64-slice computed tomography coronary angiography in patients with high, intermediate, or low pretest probability of significant coronary artery disease. J Am Coll Cardiol. 2007; 50:1469–1475. [PubMed: 17919567]

6. Achenbach S, Moselewski F, Ropers D, Ferencik M, Hoffmann U, MacNeill B, Pohle K, Baum U, Anders K, Jang I, Daniel W, Brady T. Detection of calcified and noncalcified coronary atherosclerotic plaque by contrast-enhanced, submillimeter multidetector spiral computed tomography: A segment-based comparison with intravascular ultrasound. Circulation. 2004; 109:14–17. [PubMed: 14691045]

7. Achenbach S, Ropers D, Hoffmann U, MacNeill B, Baum U, Pohle K, Brady TJ, Pomerantsev E, Ludwig J, Flachskampf FA, Wicky S, Jang IK, Daniel WG. Assessment of coronary remodeling in stenotic and nonstenotic coronary atherosclerotic lesions by multidetector spiral computed tomography. J Am Coll Cardiol. 2004; 43:842–847. [PubMed: 14998627]

8. Leber AW, Becker A, Knez A, von Ziegler F, Sirol M, Nikolaou K, Ohnesorge B, Fayad ZA, Becker CR, Reiser M, Steinbeck G, Boekstegers P. Accuracy of 64-slice computed tomography to classify and quantify plaque volumes in the proximal coronary system: A comparative study using intravascular ultrasound. J Am Coll Cardiol. 2006; 47:672–677. [PubMed: 16458154]

9. Leber AW, Knez A, Becker A, Becker C, von Ziegler F, Nikolaou K, Rist C, Reiser M, White C, Steinbeck G, Boekstegers P. Accuracy of multidetector spiral computed tomography in identifying and differentiating the composition of coronary atherosclerotic plaques: A comparative study with intracoronary ultrasound. J Am Coll Cardiol. 2004; 43:1241–1247. [PubMed: 15063437]

10. Pundziute G, Schuijf JD, Jukema JW, Decramer I, Sarno G, Vanhoenacker PK, Boersma E, Reiber JHC, Schalij MJ, Wijns W, Bax JJ. Evaluation of plaque characteristics in acute coronary syndromes: Non-invasive assessment with multi-slice computed tomography and invasive evaluation with intravascular ultrasound radiofrequency data analysis. European Heart Journal. 2008; 29:2373–2381. [PubMed: 18682447]

11. Herzog BA, Husmann L, Valenta I, Gaemperli O, Siegrist PT, Tay FM, Burkhard N, Wyss CA, Kaufmann PA. Long-term prognostic value of 13n-ammonia myocardial perfusion positron emission tomographyadded value of coronary flow reserve. Journal of the American College of Cardiology. 2009; 54:150–156. [PubMed: 19573732]

12. Murthy VL, Naya M, Foster CR, Hainer J, Gaber M, Di Carli G, Blankstein R, Dorbala S, Sitek A, Pencina MJ, Di Carli MF. Improved cardiac risk assessment with noninvasive measures of coronary flow reserve. Circulation. 2011; 124:2215–2224. [PubMed: 22007073]

13. Ziadi MC, deKemp RA, Williams KA, Guo A, Chow BJW, Renaud JM, Ruddy TD, Sarveswaran N, Tee RE, Beanlands RSB. Impaired myocardial flow reserve on rubidium-82 positron emission tomography imaging predicts adverse outcomes in patients assessed for myocardial ischemia. Journal of the American College of Cardiology. 2011; 58:740–748. [PubMed: 21816311]

14. Fiechter M, Gebhard C, Ghadri JR, Fuchs TA, Pazhenkottil AP, Nkoulou RN, Herzog BA, Altorfer U, Gaemperli O, Kaufmann PA. Myocardial perfusion imaging with 13n-ammonia pet is a strong predictor for outcome. Int J Cardiol. 2013; 167:1023–1026. [PubMed: 22475847]

15. Slomka PJ, Alexanderson E, Jacome R, Jimenez M, Romero E, Meave A, Le Meunier L, Dalhbom M, Berman DS, Germano G, Schelbert H. Comparison of clinical tools for measurements of regional stress and rest myocardial blood flow assessed with 13n-ammonia pet/ct. J Nucl Med. 2012; 53:171–181. [PubMed: 22228795]

16. Choi Y, Huang SC, Hawkins RA, Kuhle WG, Dahlbom M, Hoh CK, Czernin J, Phelps ME, Schelbert HR. A simplified method for quantification of myocardial blood flow using nitrogen-13-ammonia and dynamic pet. J Nucl Med. 1993; 34:488–497. [PubMed: 8280197]

17. Dey D, Cheng VY, Slomka PJ, Nakazato R, Ramesh A, Gurudevan S, Germano, Berman DS. Automated three-dimensional quantification of non-calcified and calcified coronary plaque from coronary ct angiography. Journal of Cardiovascular Computed Tomography. 2009:372–382. [PubMed: 20083056]

18. Dey D, Schepis T, Marwan M, Slomka PJ, Berman DS, Achenbach S. Automated three-dimensional quantification of non-calcified coronary plaque from coronary ct angiography: Comparison with intravascular ultrasound. Radiology. 2010; 257:516–522. [PubMed: 20829536]

19. Motoyama S, Sarai M, Harigaya H, Anno H, Inoue K, Hara T, Naruse H, Ishii J, Hishida H, Wong ND, Virmani R, Kondo T, Ozaki Y, Narula J. Computed tomographic angiography characteristics of atherosclerotic plaques subsequently resulting in acute coronary syndrome. Journal of the American College of Cardiology. 2009; 54:49–57. [PubMed: 19555840]

20. Steigner ML, Mitsouras D, Whitmore AG, Otero HJ, Wang C, Buckley O, Levit NA, Hussain AZ, Cai T, Mather RT, Smedby O, DiCarli MF, Rybicki FJ. Iodinated contrast opacification gradients in normal coronary arteries imaged with prospectively ecg-gated single heart beat 320-detector row computed tomography. Circ Cardiovasc Imaging. 2009; 3:179–186. [PubMed: 20044512]

21. Schuhbaeck A, Dey D, Otaki Y, Kral B, Slomka P, Nakazato R, Achenbach S, Berman D, Fishman E, Lai S, Lai H. Interscan reproducibility of quantitative coronary plaque volume and composition from ct coronary angiography using an automated method. Journal of the American College of Cardiology. 2013; 61doi: 10.1016/S0735-1097(1013)61040-61042

22. Friedman J, Hastie T, Tibshirani R. Additive logistic regression: A statistical view of boosting. Annals of Statistics. 2000; 28:337–407.

23. Freund Y, Schapire RE. A decision-theoretic generalization of online learning and an application to boosting. Journal of Computer and System Sciences. 1997; 55:119–139.

24. Freund Y, Schapire RE. Experiments with a new boosting algorithm. Machine Learning: Proceedings of the Thirteenth International Conference. 1998:148–156.

25. Dettling M, Buhlmann P. Boosting for tumor classification with gene expression data. Bioinformatics. 2003; 19:1061–1069. [PubMed: 12801866]

26. Arsanjani R, Xu Y, Dey D, Fish M, Dorbala S, Hayes S, Berman DS, Germano G, Slomka PJ. Improved accuracy of myocardial perfusion spect for the detection of coronary artery disease by utilizing a support vector machines algorithm. J Nucl Med. 2013; 54:549–555. [PubMed: 23482666]

27. Witten, IH.; Frank, E.; Hall, MA. Data mining: Practical machine learning tools and techniques, third edition. Burlington, MA: Morgan Kaufmann Publishers; 2011.

28. Molinaro AM, Simon R, Pfeiffer RM. Prediction error estimation: A comparison of resampling methods. Bioinformatics. 2005; 21:3301–3307. [PubMed: 15905277]

29. Chiribiri A, Hautvast GL, Lockie T, Schuster A, Bigalke B, Olivotti L, Redwood SR, Breeuwer M, Plein S, Nagel E. Assessment of coronary artery stenosis severity and location: Quantitative analysis of transmural perfusion gradients by high-resolution mri versus ffr. JACC Cardiovasc Imaging. 2013; 6:600–609. [PubMed: 23582358]

30. [Accessed July 21, 2015] Http://www.Stata.Com/manuals13/rvce_option.Pdf#rvce_option.2015

31. [Accessed July 21, 2015] Http://www.Stata.Com/manuals13/rlogistic.Pdf.2015

32. DeLong ER, DeLong DM, Clarke-Pearson DL. Comparing the areas under two or more correlated receiver operating characteristic curves: A nonparametric approach. Biometrics. 2007; 44:837–845. [PubMed: 3203132]

33. Shmilovich H, Cheng VY, Tamarappoo BK, Dey D, Nakazato R, Gransar H, Thomson LE, Hayes SW, Friedman JD, Germano G, Slomka PJ, Berman DS. Vulnerable plaque features on coronary ct

angiography as markers of inducible regional myocardial hypoperfusion from severe coronary artery stenoses. Atherosclerosis. 2011; 219:588–595. [PubMed: 21862017]

34. Greiner M, Sohr D, Gobel P. A modified roc analysis for the selection of cut-off values and the definition of intermediate results of serodiagnostic tests. J Immunol Methods. 1995; 185:123–132. [PubMed: 7665894]

35. Naya M, Murthy VL, Foster CR, Gaber M, Klein J, Hainer J, Dorbala S, Blankstein R, Di Carli MF. Prognostic interplay of coronary artery calcification and underlying vascular dysfunction in patients with suspected coronary artery disease. J Am Coll Cardiol. 2013; 61:2098–2106. [PubMed: 23524053]

36. Murthy VL, Naya M, Taqueti VR, Foster CR, Gaber M, Hainer J, Dorbala S, Blankstein R, Rimoldi O, Camici PG, Di Carli MF. Effects of sex on coronary microvascular dysfunction and cardiac outcomes. Circulation. 2014; 129:2518–2527. [PubMed: 24787469]

37. Kajander S, Joutsiniemi E, Saraste M, Pietila M, Ukkonen H, Saraste A, Sipila HT, Teras M, Maki M, Airaksinen J, Hartiala J, Knuuti J. Cardiac positron emission tomography/computed tomography imaging accurately detects anatomically and functionally significant coronary artery disease. Circulation. 2010; 122:603–613. [PubMed: 20660808]

38. Naya M, Murthy VL, Blankstein R, Sitek A, Hainer J, Foster C, Gaber M, Fantony JM, Dorbala S, Di Carli MF. Quantitative relationship between the extent and morphology of coronary atherosclerotic plaque and downstream myocardial perfusion. Journal of the American College of Cardiology. 2011; 58:1807–1816. [PubMed: 21996395]

39. Diaz Zamudio M, Dey D, Schuhbaeck A, Nakazato R, Slomka PJ, Bermand DS, Achenbach S, Min JK, Doh JH, Koo BK. Automated quantitative plaque burden from coronary ct angiography noninvasively predicts hemodynamic significance by fractional flow reserve in intermediate coronary lesions. Radiology. 2015 Apr 17.:141648. [Epub ahead of print].

40. Davignon J, Ganz P. Role of endothelial dysfunction in atherosclerosis. Circulation. 2004; 109:III27–32. [PubMed: 15198963]
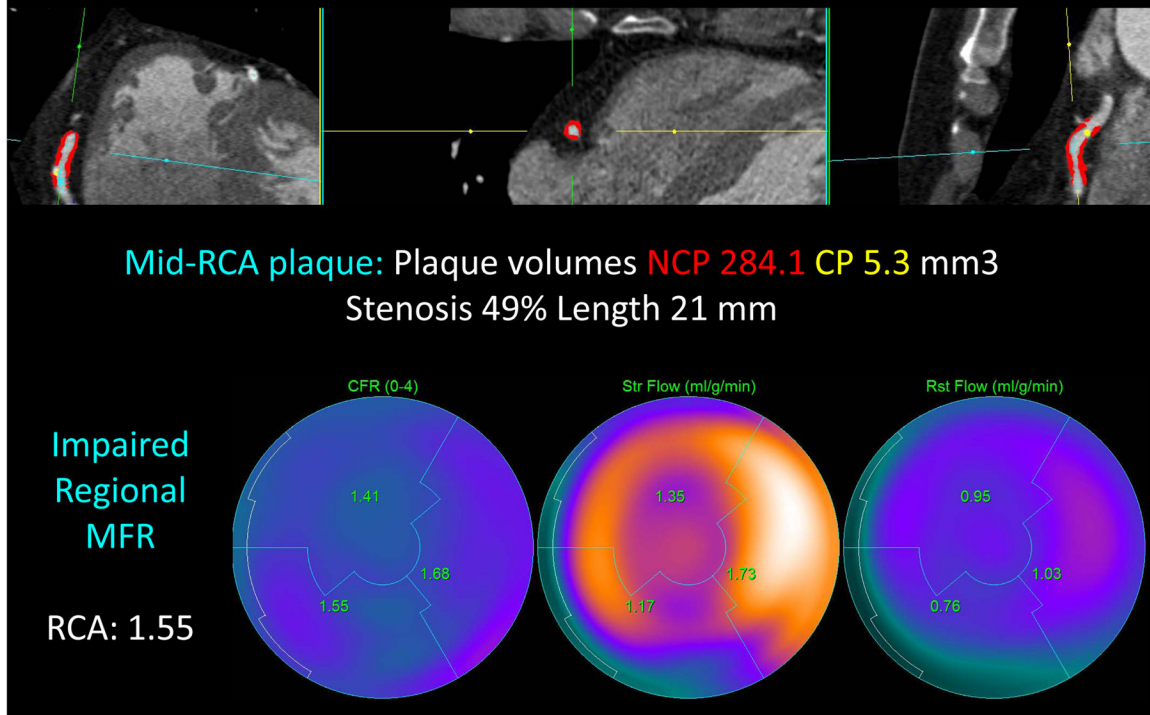
Figure 1.
Case example from our study: for a 50-year old male patient with multiple risk factors including diabetes, hypertension and family history. Top row shows RCA coronary artery with non-calcified plaque in red overlay and calcified plaque in yellow overlay. Bottom row shows impaired regional MFR (1.55 for the RCA territory)
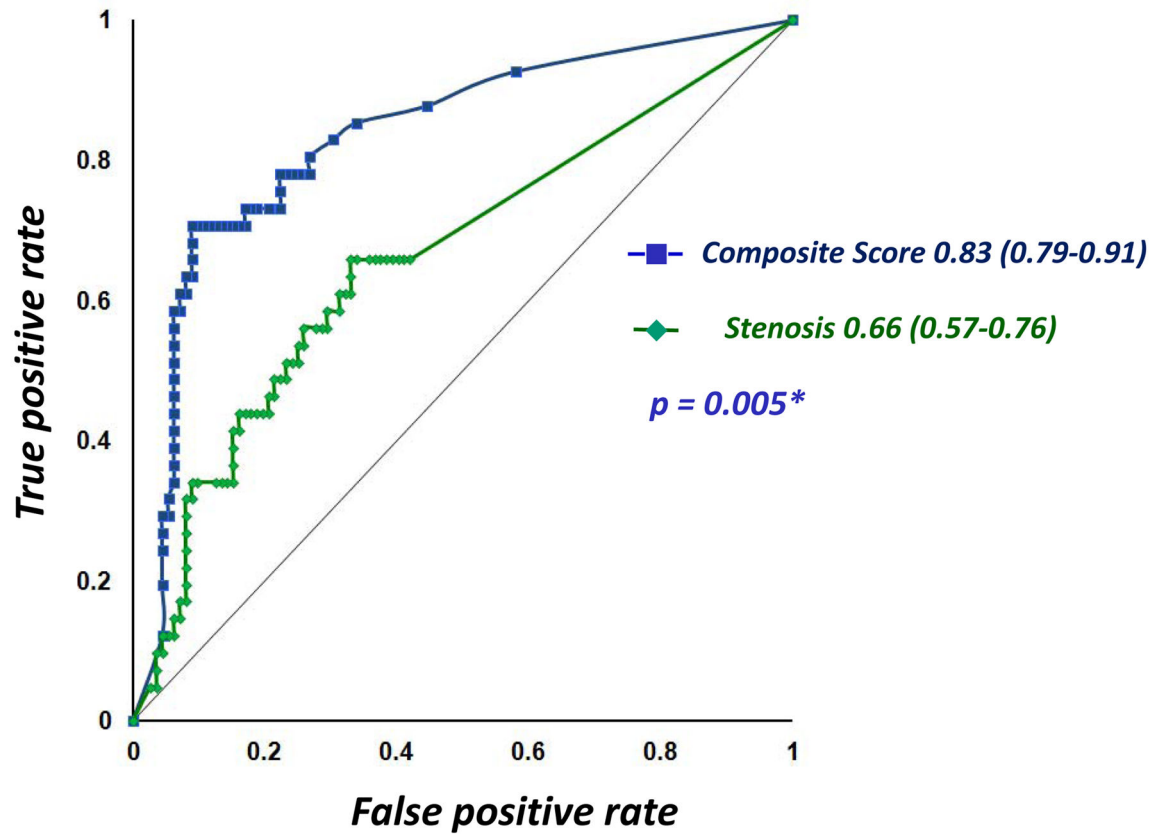
Figure 2.
Receiver-Operator Analysis for the composite risk score and maximum diameter stenosis (per-vessel). For prediction of impaired MFR, ROC-Area-under-the-curve for the composite risk score was 0.83 (95% CI: 0.79–0.91), significantly higher than for quantitative stenosis (0.66, 95% CI: 0.57–0.76, p = 0.005).

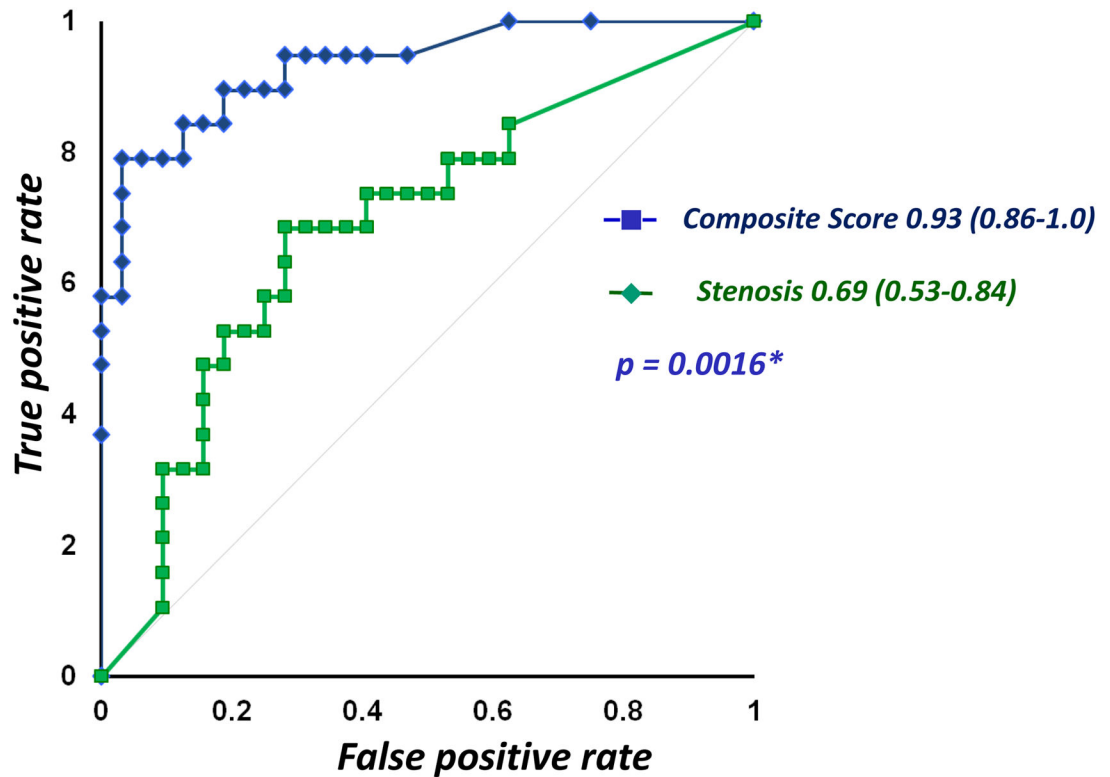## Prediction of impaired MFR by coronary CTA (per-patient) 51 patients

Figure 3.

Receiver-Operator Analysis for the composite risk score and maximum diameter stenosis (per-patient). For prediction of impaired MFR, ROC-Area-under-the-curve for the composite risk score was 0.93 (95% CI: 0.86–1.0), significantly higher than for quantitative stenosis (0.69, 95% CI: 0.53–0.84, p = 0.0016).

Table 1

Patient Characteristics (51 patients)

	Mean (SD)
Age (in years)	63 ±9
Gender (men, **%**)	32 (63)
Weight (in Kg)	75 ± 14
BMI (in kg/m2)	27.3 ± 3.7
Systolic blood pressure (mm Hg)	125 ± 16
Diastolic blood pressure (mm Hg)	81 ± 8
Heart rate (beats per minute)	68 ± 9
Risk factors (N, %)	
Diabetes	16 (31)
Hypertension	27 (53)
Dyslipidemia	32 (63)
Current smoker	12 (24)
Previous smoker	10(20)
Family history	15 (29)
Three or more risk factors	26 (51)
Known CAD	12 (24)
History of MI	1 (2)
Symptoms **(%)**	
Typical chest pain	15(29)
Atypical chest pain	10 (20)
Dyspnea	12(24)

Table 2

Stress and rest myocardial blood flow in all patients and in patients with impaired and normal MFR

	All patients (51 patients)	Normal MFR (32 patients)	Impaired MFR (19 patients)	p-value
Stress Myocardial Blood Flow (ml/g/min)	2.2±0.8	2.4±0.8	1.7±0.7	**<0.0001**
Rest Myocardial Blood Flow (ml/g/min)	0.8±0.3	0.8±0.2	1.0±0.4	**<0.0001**

Table 3

Quantitative adverse plaque features in patients with normal and impaired regional MFR (153 vessels).

	Normal MFR	Impaired MFR	p
Maximum diameter stenosis (%)	19.5 ±28.1	38.3 ±33.9	**0.010**
Total plaque volume (mm^3)	118 ±211	254 ±351	0.276
Non-calcified plaque volume (mm^3)	100 ±171	209 ±266	0.115
Low-density non-calcified plaque volume (mm^3)	23.5 ±42.8	45.2 ±58.2	0.107
Calcified plaque volume (mm^3)	17.9 ±60.5	44.5 ±102.5	0.624
Total plaque burden	19.3 ±26.4	37 ±30.9	**0.007**
Non-calcified plaque burden (%)	17.2 ±24.6	32.4 ±27	**0.006**
Low-density non-calcified plaque burden (%)	4.0 ±6.2	7 ±7.2	**0.015**
Calcified plaque burden (%)	2.0 ±4.9	4.6 ±8.5	0.987
Remodeling index	1.1 ±0.4	1.2 ±0.8	0.992
Total lesion length (mm)	14 ±23.6	27.5 ±27	0.485
Contrast density difference (%)	8.4 ±14.8	17.9 ±20.9	**0.006**

Table 4

Univariate logistic regression of quantitative adverse plaque features for prediction of regional impaired MFR.

Quantitative plaque features	Odds Ratio (95% CI)	P
Number of risk factors	0.9 (0.6–1.4)	0.75
Non calcified plaque burden	**1.35 (1.1–1.75)**	**0.02**
Low-density plaque burden	**1.54 (1.1 – 2.2)**	**0.03**
Calcified plaque burden	1.36 (0.9–2.1)	0.18
Total plaque burden	**1.33 (1.1–1.7)**	**0.025**
Maximum diameter stenosis	**1.34 (1.1–1.7)**	**0.03**
Contrast density difference	**1.45 (1.1–2.0)**	**0.016**
Lesion length	**1.37 (1.1–1.8)**	**0.03**

Table 5

Multivariable logistic regression analysis of quantitative adverse plaque features for regional impaired MFR.

Quantitative plaque features	Odds Ratio (95% CI)	P
Non calcified plaque burden	**1.35 (1.1–1.75)**	**0.021**
Maximum diameter stenosis	-	0.77
Lesion length	-	0.96

Table 6

Spearman rank correlations for quantitative adverse plaque features with regional MFR and stress myocardial blood flow values.

Quantitative adverse plaque features	Correlation with regional MFR	P	Correlation with regional stress MBF	P
Non calcified plaque burden	−0.34	**<0.0001**	−0.28	**0.003**
Calcified plaque burden	−0.26	**0.002**	−0.40	**<0.0001**
Total plaque burden	−0.37	**<0.0001**	−0.32	**0.0007**
Low-density non-calcified plaque burden	−0.28	**0.0008**	−0.28	**0.002**
Stenosis	−0.39	**<0.0001**	−0.37	**0.0001**
Contrast density difference	−0.37	**<0.0001**	−0.35	**0.0002**
Lesion length	−0.35	**<0.0001**	−0.40	**<0.0001**